

FAIR-BFL: Flexible and Incentive Redesign for Blockchain-based Federated Learning*

Rongxin Xu

Hunan Key Laboratory of Data Science & Blockchain,
Business School, Hunan University
Changsha 410082, China
rongxinxu@hnu.edu.cn

Qiujun Lan

Hunan Key Laboratory of Data Science & Blockchain,
Business School, Hunan University
Changsha 410082, China
lanqiujun@hnu.edu.cn

Shiva Raj Pokhrel[†]

School of IT, Deakin University
Geelong, VIC 3216, Australia
shiva.pokhrel@deakin.edu.au

Gang Li

Centre for Cyber Security Research and Innovation,
Deakin University
Geelong, VIC 3216, Australia
gang.li@deakin.edu.au

ABSTRACT

Vanilla *Federated learning* (FL) relies on the centralized global aggregation mechanism and assumes that all clients are honest. This makes it a challenge for FL to alleviate the *single point of failure* and dishonest clients. These impending challenges in the design philosophy of FL call for blockchain-based federated learning (BFL) due to the benefits of coupling FL and blockchain (e.g., democracy, incentive, and immutability). However, one problem in vanilla BFL is that its capabilities do not follow adopters' needs in a dynamic fashion. Besides, vanilla BFL relies on unverifiable clients' self-reported contributions like data size because checking clients' raw data is not allowed in FL for privacy concerns. We design and evaluate a novel BFL framework, and resolve the identified challenges in vanilla BFL with greater flexibility and incentive mechanism called *FAIR-BFL*. In contrast to existing works, *FAIR-BFL* offers unprecedented flexibility via the modular design, allowing adopters to adjust its capabilities following business demands in a dynamic fashion. Our design accounts for BFL's ability to quantify each client's contribution to the global learning process. Such quantification provides a rational metric for distributing the rewards among federated clients and helps discover malicious participants that may poison the global model.

KEYWORDS

Federated Learning, Blockchain, Incentive, Security and Privacy

1 INTRODUCTION

The advent of *federated learning* (FL) [8] has ameliorated the shortcomings of the centralized ML techniques, which were caused by the ever-increasing data scale and model complexity. FL addresses the concerns on data ownership and privacy by ensuring that no raw data leave the distributed end devices (also referred to as clients). It successfully employs a single global server in a distributed system to collect updates from end devices [21]. FL performs the renewal aggregation and iteratively distributes new global learning

model to the clients. However, such a FL setup based on centralized server suffers from issues such as *single point of failure* and instability [22]. Moreover, attacks against distributed training of FL have revealed that malicious or compromised clients/central servers may upload modified global parameters, causing model poisoning, because attackers can forge local updates to launch inference attacks [16]. Therefore, the design of a robust FL mechanism is essential to the stability and security of distributed computing systems.

As a proven decentralized framework, blockchain naturally ponders the benefits of merging with FL [17], including immutability, traceability, and incentive mechanisms, let alone the fact that both blockchain and FL are inherently distributed by nature. Several recent works have been proposed to empower FL's robustness, intelligence, and privacy-preserving capabilities by incorporating blockchain. *Blockchain-based Federated Learning* (BFL), proposed in [21], has been considered as one promising and celebrated approach to facilitating distributed computing and learning. Notable studies along this line of research include [18–21]. In BFL, local updates and global models can be recorded through the blockchain to ensure security, and clients would automatically acquire new global parameters through a consensus mechanism. However, BFL requires flexibility because adopters' needs are dynamic, e.g., when business shrinks, adopters may expect to quickly switch from BFL to degraded versions (FL or blockchain) for the sake of cost reduction. Moreover, blockchain rewards those nodes that win the mining competition, but in BFL, we desire to attract potential participants and keep clients who make great contributions to global updates. Therefore, BFL also needs a novel incentive mechanism. Unfortunately, existing works have not adequately studied the flexibility and incentive mechanism in BFL, which we refer to as vanilla BFL, thus it is difficult for them to move toward practical use. There exist three more challenges in moving vanilla BFL towards flexibility and effective incentive.

Tightly coupling blockchain and FL FL has a periodic learning-updating-waiting process while the blockchain keeps running. In vanilla BFL, these two play almost independently,

*To appear in ICPP '22

[†]Corresponding Author

thus posing severe concerns. One prevalent concern is unwanted consequences such as “*forking is inevitable*” [21]. Ameliorating the impact of forking (as studied in [3, 13]) is non-trivial as it often loses some local updates and adversely impacts global learning. It becomes intractable when local updates recorded in the block can not reflect the actual FL stage and generates empty blocks [2]. Therefore, it is crucial to tightly couple both blockchain and FL in BFL, especially to coordinate miners’ behavior.

Defining block’s data scope All nodes in the blockchain network have access to the data in the block, so any data which may reveal the privacy must be avoided from being made public. As the block size is limited, vanilla BFL may generate more blocks because it records all the data to complete the same round of learning. Moreover, each block results from a round of mining competition, and large blocks can increase the transfer time. Thus, the delay of vanilla BFL can be high. So the data recorded in the block should be carefully defined to reduce the delay of BFL.

Incentivizing based on contribution Blockchain can provide incentives for FL, whereas it rewards those miners that successfully mine blocks. BFL desires to reward clients who contribute more to the global aggregation to attract potential participants, especially in data-intensive tasks. To this end, a method is needed to help BFL differentiate the client contributions. At the same time, such a method should not rely on clients’ self-reported contributions. Otherwise, clients could have good reasons to cheat, and the BFL cannot verify who are dishonest since the limitation in checking the client’s raw data. Unfortunately, vanilla BFL mainly relies on the client’s self-reporting contributions or checking raw data to determine rewards.

Therefore, flexibility and effective incentive should be considered in BFL to fully move towards practical use. It requires enhancing vanilla BFL with a tightly coupled framework and contribution-based incentive mechanism to improve performance and security. The above challenges motivate us to develop new insights in designing the BFL framework. To this end, we propose *FAIR-BFL*, a novel BFL framework with *flexible and incentive redesign*, which mitigates the above-mentioned issues in vanilla BFL, and our main contributions can be summarized as follows:

- (1) We develop new insights in designing blockchain-based federated learning framework by coordinating miners’ behavior, recording the desirable global gradients, thus, jointly improving the flexibility and enhancing performance-cum-security.
- (2) We propose a contribution-based incentive mechanism that supports quantifying each client’s contribution with various clustering algorithms, defending against malicious attacks, and selecting high-contributing clients to speed up model convergence.
- (3) With the incentive mechanism in *FAIR-BFL*, we propose an aggregation method to assign clients’ weights based on their contributions, which improves the performance considerably with guaranteed fairness and convergence.

The rest of this paper is organized as follows. We start with Section 2, which provides background knowledge on BFL, related work, and challenges faced by vanilla BFL. Then, we propose *FAIR-BFL* in Section 3 and show how it overcomes the challenges with several novel insights. In Section 4, we reveal how *FAIR-BFL* provides unprecedented flexibility through functional scaling and analyze its performance. After that, we move to experiments in Section 5 to demonstrate the performance, latency, and security of *FAIR-BFL*. Finally, Section 6 concludes this work.

2 BACKGROUND AND RELATED WORK

Blockchain maintains a distributed ledger to securely record conclusive information (called *block*), in which the nodes compete for bookkeeping in a mining competition and reach agreement through a consensus mechanism. The newly generated block is broadcasted in the network, and those who receive the message will stop their current computation.

FL employs a distributed learning which allows end devices to train their own models locally and then aggregates intermediate information to provide global insights by using local learnings at a central server. It aims to solve the problem of *data island*¹ and benefit from aggregate modelling. Specifically, at the beginning of each communication round, the clients update their local models with their data and upload the obtained gradients to the central server. After that, the central server computes the global updates by aggregating all received local gradients and supplies the global gradients to the clients. Finally, the clients apply the global gradients to update their local models independently. Thus, FL dynamics evolves from one round to another.

Some notable studies along the lines of BFL include [1, 11, 12, 14, 21]. Among them, Awan et al. [1] designed a variant of the *Pailier* cryptosystem to support additional homomorphic encryption and proxy re-encryption, so that the privacy of the transmission is protected in the BFL. Majeed and Hong [14] adopted the concept of “channels” in their BFL framework, *FLchain*, to store the gradient of the local model in the block of a channel. Components such as *Ethereum*, extend the capability of *FLchain* in executing the global updates. Lu et al. [12] incorporated federated learning with differential privacy into permissioned blockchain to alleviate the centralized trust problem. Li et al. [11] applied the blockchain to store the global model and exchange the local updates, thus eliminating the central server and resisting privacy attacks from malicious clients and central server, it also reduces the computation time using committee-based consensus.

The aforementioned works developed the vanilla BFL framework for better privacy and data security. However, vanilla BFL design still faces some non-trivial challenges. For example, the asynchronous nature of blockchain requires in-depth integration into

¹Imagine data as a flowing ocean from which some entities collect data and keep it locally rather than sharing it, e.g., financial institutions. Thus, these stagnant data become islands one after another.

the FL's communication rounds mechanism. In vanilla BFL frameworks, blockchain and federated learning are more like two separate parts that are unnecessarily aligned in terms of their working states, making it problematic to ensure coherent BFL operations. Moreover, in most existing vanilla BFL frameworks, objective evaluation of the client's contribution has been considered as irrelevant, while recording all local updates in a few of them [7, 21] arose serious privacy leakage concerns. None of the aforementioned works focus on the *flexibility and incentive mechanism of the BFL by design*. In this paper, we propose *FAIR-BFL* with a modular design, novel insights, a fairer aggregation scheme and a contribution-based incentive mechanism, thus jointly enhancing the performance and the security.

3 FLEXIBLE AND INCENTIVE REDESIGN FOR BFL

In this section, we propose *FAIR-BFL* and develop the algorithm in detail, and then we demonstrate how to integrate blockchain and FL tightly by utilizing their internal working principles. Table 1 summarizes all the notations used in this paper.

Table 1: Summary of notations

Notations in this work	
C_i	The client i in BFL and FL, or a worker in blockchain.
S_k	The miner k in BFL and blockchain, or a server in FL.
\mathcal{D}	The Data set we used
λ	The ratio of randomly selected clients in each round
η	The learning rate of the model we use
E	The number of epochs of the client's local model
B	The batch size of client's local model
n	The number of clients or workers
m	The number of miners
\mathcal{B}	Sub-data sets divided by batch size
w	The gradient in FL or BFL

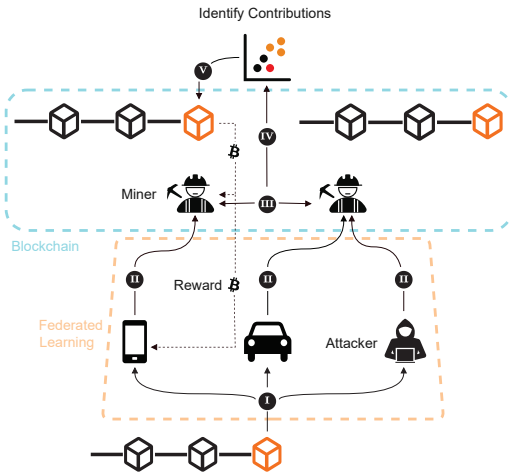


Figure 1: The framework of FAIR-BFL

Algorithm 1 FAIR-BFL Algorithm

```

1: Initialization:  $\{C_i\}_{i=1}^n, \{S_k\}_{k=1}^m, \mathcal{D}, \lambda, \eta, E, B$ 
2: for each round  $r = 1, 2, 3, \dots$  do
3:    $\{C_i\}_{i=1}^{\lambda n} \leftarrow \text{Randomly select } \lambda n \text{ } C_i \in \{C_i\}_{i=1}^n$ 
4:   for all  $C_i \in \{C_i\}_{i=1}^{\lambda n}$  do
5:     allocate  $\mathcal{D}_i \sim \mathcal{D}$  to  $C_i$ 
6:     procedure LOCAL MODEL UPDATE( $C_i, \mathcal{D}_i, B, E$ )
7:       read global gradient  $w_r$  from the latest block
8:        $\mathcal{B} \leftarrow \text{split } \mathcal{D}_i \text{ into batches of size } B$ 
9:       for each epoch  $i$  from 1 to  $E$  do
10:        for each batch  $b \in \mathcal{B}$  do
11:           $w_{r+1}^i \leftarrow w_r^i - \eta \nabla \ell(w_r^i; b)$ 
12:        procedure UPLOAD LOCAL GRADIENTS( $C_i, w_{r+1}^i, S_k$ )
13:          randomly associate  $C_i$  to  $S_k$ 
14:          upload updated gradient  $w_{r+1}^i$  to  $S_k$ 
15:        for all  $S_k \in \{S_k\}_{k=1}^m$  do
16:          procedure EXCHANGE GRADIENTS( $\{w_{r+1}^i\}, S_k$ )
17:             $W_{r+1}^k \leftarrow \{w_{r+1}^i, i = \text{index of associate clients}\}$ 
18:            broadcast clients updated gradient  $W_{r+1}^k$ 
19:            received updated gradient  $W_{r+1}^v$  from  $S_v$ 
20:            for  $w \in W_{r+1}^v$  do
21:              if  $w \notin W_{r+1}^k$  then
22:                 $W_{r+1}^k$  append  $w$ 
23:            procedure COMPUTING GLOBAL UPDATES( $W_{r+1}^k, S_k$ )
24:               $w_{r+1} \leftarrow \frac{1}{n} \sum_{i=1}^n w_{r+1}^i, w_{r+1}^i \in W_{r+1}^k$   $\triangleright$  Simple
                Average
25:               $W_{r+1}^k$  append  $w_{r+1}$ 
26:              Contribution-based Incentive Mechanism( $W_{r+1}^k$ )
27:              Fair Aggregation( $W_{r+1}^k$ )  $\triangleright$  By Equation (1)
28:            procedure BLOCK MINING AND CONSENSUS( $w_{r+1}, S_k$ )
29:              do proof of work
30:              if hash satisfies target then
31:                 $Trans. \leftarrow \text{reward list}$ 
32:                generate and add  $\text{block}(Trans., w_{r+1})$ 
33:                broadcast
34:              if received  $\text{block}_i$  then
35:                verify proof of work
36:                if hash satisfies target then
37:                  stop current proof of work
38:                  blockchain add  $\text{block}_i$ 

```

A high-level view of *FAIR-BFL* framework is shown in Figure 1, in which the circled number indicates the corresponding procedure defined and explained in Algorithm 1 and Section 4. We summarize the entire process of BFL into five procedures that interact among different entities: i) the client reads the global parameters from the latest block and updates its local model; ii) the client connects to a miner and uploads its local model; please note that some clients may be malicious; iii) miners exchange gradient sets

and start the mining competition; iv) the winner identifies the contributions and computes the global updates, and this will help disregard the information forged by the attackers due to low contribution; v) the winner packs the global update and reward information into a new block, and then all miners reach an agreement through the consensus mechanism. More specifically, the whole process is a holistic approach with multiple rounds of communication among n clients $\{C_i\}_{i=1}^n$ with a set of m miners $\{S_k\}_{k=1}^m$ to handle the blockchain process. We then utilize data set \mathcal{D} , by assuming that the sub dataset \mathcal{D}_i is at the client C_i before the start of each communication round.

3.1 Coupled BFL design

Vanilla BFL design faces some challenges in flexibility and privacy [21]. On the one hand, the workflows of FL and blockchain are inconsistent in the vanilla BFL. Hence, miners will continue to compete for excavation without stopping, which undoubtedly increases resource consumption. For example, if a miner does not receive any gradient update but completes the hash puzzle ahead of other miners, it will generate an empty block, which does not benefit the FL part. However, [4] have shown that performing SGD based on communication rounds in FL is better than asynchronous methods. To this end, we bring it into BFL to achieve the tight coupling between blockchain and FL, also alleviate issues such as forking, empty blocks, and resource cost. Note that Assumption 1 has been made in [7], but only to simplify the problems for analysis. We have the following Assumption 1.

ASSUMPTION 1 (TIGHT COUPLING). *Clients and miners are fully synchronized in every communication rounds.*

On the other hand, vanilla BFL records every local gradient in the blockchain, and workers read the block's information to calculate the global updates themselves. In this case, vanilla BFL is a white-box for the attacker, malicious nodes can use this information to perform privacy attacks and easily track the changes in a worker's local gradient to launch more severe model inversion attacks [6]. Furthermore, imagining the BFL applications in large-scale scenarios, where thousands of local gradients could be waiting for miners to pack. However, the block size is limited due to the communication cost and delay, and many local gradients will miss the current block. Eventually, to calculate the global gradient, workers have to wait for a new block to be generated until all local gradients have been recorded in the blockchain, which undoubtedly increases the latency and the communication costs. To address the concerns we have the following Assumption 2.

ASSUMPTION 2 (BOUNDING BLOCK'S DATA SCOPE). *Miners pack only the global gradients into blocks. In the end, each block contains only the global gradient of a specific round.*

Observe that Assumption 2 is to bound the block's data scope, also protects the security of FAIR-BFL and alleviates the transaction queuing caused by the limitation of block size in the asynchronous design. To the best of our knowledge, this is the first attempt to use Assumption 2 in the BFL design and validate its capability.

Algorithm 2 Client's Contribution Identification Algorithm

Input: W_{r+1}^k , *model name*, *Strategy*

```

1: Group List  $\leftarrow$  Clustering(model name,  $W_{r+1}^k$ )
2: for  $l_i \in$  Group List do
3:   if  $w_{r+1} \in l_i$  then
4:     for  $w_{r+1}^i \in l_i$  do
5:        $\theta_i \leftarrow$  Cosine Distance( $w_{r+1}^i$ ,  $w_{r+1}$ )
6:       Label  $C_i$  as high contribution
7:       Append  $\langle C_i, \theta_i / \sum_{k=1}^{\lambda n} \theta_k * \text{base} \rangle$  to reward list
8:   if  $w_{r+1} \notin l_i$  then
9:     for all  $w_{r+1}^i \in l_i$  do
10:      Label  $C_i$  as low contribution
11:  $W_{r+1}^k \leftarrow$  Strategy(reward list,  $W_{r+1}^k$ )

```

Output: *reward list*, W_{r+1}^k

3.2 Accounting Client's Contribution

Algorithm 2 implements our method to identify contributions in Line 26 of Algorithm 1. Various clusters of gradients are found by applying a clustering algorithm on W_{r+1}^k ; moreover, they imply different contributions. Note that any suitable clustering algorithm can be used here as needed. However, we use DBSCAN in experiments by default because it is efficient and straightforward. Those clients belonging to the same cluster as the global gradient can be considered a high contribution and be rewarded, while those far from the global gradient can be considered a low contribution and adopt a predetermined strategy. There are two strategies: i) keep all gradients; ii) discard low-contributing local gradients and recalculate the global updates w_{r+1} . The *cosine* distance θ_i (the larger the θ , the farther the distance.) between its local gradient and the global update is calculated as the weight of its contribution to the global update for a high contributing client C_i . We can set a *base* and multiply it by $\theta_i / \sum_{k=1}^{\lambda n} \theta_k$ as the final reward for client C_i . Key-value pairs $\langle C_i, \theta_i / \sum_{k=1}^{\lambda n} \theta_k * \text{base} \rangle$ represent the reward information, and they are recorded in the *reward list*. Eventually, when a miner generates a new block, the reward is distributed according to the *reward list* and appended to the current block as transactions. After the blockchain consensus is achieved, clients will get these rewards. We explain the intuition behind Algorithm 2 as follows.

Privacy preservation Vanilla BFL requires clients to report their data dimensions for rewards determination. Therefore, clients have sufficient motivation to cheat for more rewards. We cannot recognize this deception because it is impossible to check the actual data set, which violates FL's guidelines. On the contrary, as the intermediate information, the gradients can reflect both the data size and the data quality. Using them to perform Algorithm 2 can provide a more objective assessment and ensure privacy.

Malicious attack resistance Malicious clients may upload fake local gradients to attack the global model. The clustering algorithm can find these fake gradients because they are different from the real ones [16]. We can employ the discarding strategy to avoid skewing the global model with these spurious gradients, ultimately maintaining the security of FAIR-BFL.

Clients selection If we adopt the discarding strategy, at the same time, the corresponding workers will no longer participate before the round. In this respect, this approach can also be considered as a new method of clients selection, rather than simply random selection.

We will thoroughly evaluate our contribution-based incentive approach in Section 5.

3.3 Fair Aggregation

The optimization problem considered by FAIR-BFL is

$$\min_w \left\{ F(w) \triangleq \sum_{i=1}^n p_i F_i(w) \right\},$$

where $F_i(w)$, p_i are the local objective function and weight of clients i , respectively. Consider the simple average aggregation, which means $p_1 = p_2 = \dots = p_n = \frac{1}{n}$:

$$w_{r+1} \leftarrow \frac{1}{n} \sum_{i=1}^n w_{r+1}^i$$

This is simple average aggregation that treats all clients' gradients equally and averages them. However, clients may not have same sample sizes. Thus, simple averaging does not reflect such a contribution difference. Instead, we use the following method to aggregate the global gradients for fairness.

$$w_{r+1} \leftarrow \frac{1}{\lambda} \sum_{i=1}^n p_i w_{r+1}^i, \text{ where } p_i = \theta_i / \sum_{k=1}^{\lambda n} \theta_k \quad (1)$$

That is, we assign aggregation weights based on the contribution of clients to avoid model skew and improve accuracy. At the same time, it is impractical to require all devices to participate in the learning process [5, 24], so we assume that all devices are activated before the communication round begins. However, only some devices are selected to upload local gradients.

Although we use fairness aggregation and partial participation, we can still reveal the stability and convergence dynamics of FAIR-BFL. For tractability, we have used the following four well-known assumptions in literature [9, 10, 23, 26].

ASSUMPTION 3 (L-SMOOTH). Consider $F_i(w) \triangleq \frac{1}{n} \sum_{i=1}^n \ell(w; b_i)$ and F_i is L -smooth, then for all v and w ,

$$F_i(v) \leq F_i(w) + (v - w)^T \nabla F_i(w) + \frac{L}{2} \|v - w\|_2^2.$$

ASSUMPTION 4 (μ -STRONGLY). F_i is u -strongly convex, for all v and w ,

$$F_i(v) \geq F_i(w) + (v - w)^T \nabla F_i(w) + \frac{\mu}{2} \|v - w\|_2^2.$$

ASSUMPTION 5 (BOUNDED VARIANCE). The variance of stochastic gradients in each client is bounded by:

$$\mathbb{E} \left\| \nabla F_i(w_r^i, b_i) - \nabla F_i(w_r^i) \right\|^2 \leq \sigma_i^2$$

ASSUMPTION 6 (BOUNDED STOCHASTIC GRADIENT). The expected squared norm of stochastic gradients is uniformly bounded, thus for all $i = 1, \dots, n$ and $r = 1, \dots, r - 1$, we have

$$\mathbb{E} \left\| \nabla F_i(w_r^i, b_i) \right\|^2 \leq G^2$$

Assumptions 3 and 4 are essential for analyzing the convergence [9, 23, 26]. Both Assumptions 3 and 4 mandate requirements on the fundamental properties of the loss function. That is, the function does not change too fast (Assumption 1) or too slow (Assumption 2). Assumptions 5 and 6 are made in [10]. They enable us to use $w - w^*$ to approximate $F - F^*$.

THEOREM 3.1. Given Assumptions 1 to 6 hold, Algorithm 1 converges as follows

$$\mathbb{E} [F(\bar{w}_r)] - F^* \leq \frac{\kappa}{\gamma + r} \left(\frac{2(B + C)}{\mu} + \frac{\mu(\gamma + 1)}{2} \|w_1 - w^*\|^2 \right) \quad (2)$$

where $\kappa = \frac{L}{\mu}$, $\gamma = \max\{8\kappa, E\}$, the learning rate $\eta_r = \frac{2}{\mu(\gamma+r)}$, and $C = \frac{4}{\kappa} E^2 G^2$.

Equation (2) shows that the distance between the actual model F and the optimal model F^* decreases with increasing communication rounds. FAIR-BFL can converge regardless of the data distribution because we did not make an IID assumption, and it establishes the condition that guarantees the convergence of Algorithm 1. The detailed proof of Theorem 3.1 is provided in Appendix A, which is further supported by the experimental results in Section 5.

4 FLEXIBILITY BY DESIGN

We re-examined the entire process of vanilla BFL and identified the opportunity to achieve flexibility. More specifically, apart from the necessary work in the preparation phase, we divide the remaining part into five procedures, as shown in Algorithm 1. Depending on the application's needs, these five procedures can be coupled flexibly and dynamically. We present these procedures in detail and reveal this flexibility, and we further determine the possible delays in each link to model approximate performance.

4.1 Local Learning and Update

At the beginning of round $r + 1$, each client reads the global gradient w_r (if any exists) from the last block in the blockchain, and updates the local model with w_r . Next, the allocated sub-data sets \mathcal{D}_i will be divided according to the specified batch size B . For each epoch $i \in \{1, 2, 3, \dots, E\}$, the client C_i obtains the gradient w_{r+1}^i of round $r + 1$ by performing the SGD, as shown in Equation (3), where ℓ and η are the loss function and the learning rate, respectively.

$$w_{r+1}^i \leftarrow w_r^i - \eta \nabla \ell(w_r^i; b) \quad (3)$$

Equation (3) can be calculated $\frac{\mathcal{D}_i}{B}$ times with the specified batch size B . Therefore, the time complexity of eq. (3) is $O(E * \frac{\mathcal{D}_i}{B})$. Furthermore, we define the calculation time of this step as the delay

\mathcal{T}_{local} . However, please note that E and B are set as small constants for all clients under normal circumstances, so the time complexity of eq. (3) is linear $O(n)$. The learning rate η is often a more concerning issue, as it will significantly affect the performance and the convergence rate. We will explore the impact of the learning rate on *FAIR-BFL* in section 5.2.2.

4.2 Uploading the gradient for mining

After the Procedure-I, the client C_i will get the updated gradient w_{r+1}^i of round $r+1$ and upload it to the miners. There are multiple miners in the network, and they will pack gradients into blocks. In addition, BFL miners also need to play a role similar to the central server. The client does not have to contact all the miners, which will increase the communication cost, and a better choice is that each client only uploads gradients to one miner. Here, we make the probability of selecting each miner as uniform as possible, which is determined based on the specific application scenario. Specifically, the client C_i generates the miner's index k uniformly and randomly, then it associates the miner S_k and uploads the updated gradient w_{r+1}^i .

Note that it is highly risky to directly use these local gradients for subsequent global updates without verifying, because malicious clients can easily forge the information and launch the gradient attacks [16]. To avoid this risk, we use the RSA encryption algorithm to ensure that the identities of both parties are verified. In the beginning, each client is assigned a unique private key according to its ID, and the corresponding public key will be held by the miners. The gradient information received by the miner is signed with the private key, so the information can be verified by the public key, as shown in Figure 2. Further, local gradients can be encrypted using RSA to ensure data privacy.

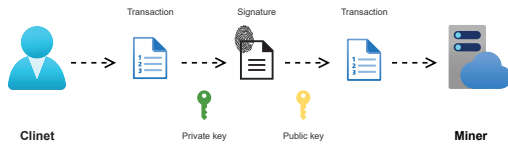


Figure 2: Miners verify transactions through RSA

The procedure will parallelly perform above steps for all clients in the current round, and the time complexity is $O(1)$. However, whether it is selecting miners or uploading gradients, the operation itself will be simple. Nevertheless, the clients are often at the edge of the network, and the quality of the channel is difficult to guarantee. It may also be subject to other external disturbances, where more significant delays are possible. For the above considerations, we regard the communication time as the main delay in this link and record it as \mathcal{T}_{up} .

4.3 Exchanging Gradients

A miner S_k , will get the updated gradient set $\{w_{r+1}^i\}$ from the associated client set $\{C_i\}$, where i is the index of the clients associated with S_k . In the meantime, each miner will broadcast its own gradient set. Note that we cancel the queuing here by Assumption 1. The

miner will check whether the received transaction exists in the current gradient set $\{w_{r+1}^i\}$, and if not, it will append this transaction. In the end, all miners have the same gradient set.

Miners will also use the RSA encryption algorithm to validate the transactions from other miners to ensure that the data has not been tampered with, as described in Figure 2. The above steps are parallel. For each miner, it does only three things: i) broadcasts the gradient set owned. ii) receives the gradient sets from other miners. iii) adds the local gradients which it does not own. That means, the time complexity of the current procedure is $O(m)$, and we denote the time required from the start to the moment when all miners have the same gradient set as \mathcal{T}_{ex} . Normally, the number of miners will be scarce, so it is easy to ensure good communications among them, which is also the need of the practical application. Under such circumstances, \mathcal{T}_{ex} is insignificant.

4.4 Computing Global Updates

So far, every miner will have all the local updates in this round. In order to obtain the global gradient w_{r+1} , they only need to perform fairness aggregation by Equation (1). So that the clients can initialize the model parameters in the $r+1$ round.

After that, to evaluate each client's contribution in this round, the global gradient w_{r+1} is appended to the current local update set W_{r+1}^k , then we perform Algorithm 2 on W_{r+1}^k to identify client contributions and issue rewards.

The current procedure only needs to compute the global gradient using Equation (1) and then perform Algorithm 2, so the time complexity depends on the clustering algorithm, represented as $O(\text{clustering})$. Also, we denote the time cost as the delay \mathcal{T}_{gl} .

4.5 Block Mining and Consensus

Once the global gradient calculation is completed, all miners will immediately enter the mining competition. Specifically, the miner will continuously change the nonce in the block header, and then calculate whether the block's hash meets the *Target* by SHA256. The whole process can be explained as Equation (4), where *Target*₁ is a large constant, representing the maximum mining difficulty. Note that *Target* is the same for all miners, and mining difficulty will be specified before the algorithm starts. Therefore, the probability that a miner obtains the right to generate blocks will depend on the speed of the hash calculation.

$$H(\text{nonce} + \text{Block}) < \text{Target} = \frac{\text{Target}_1}{\text{difficulty}} \quad (4)$$

If a miner gets the solution of Equation (4) ahead of other miners, it will immediately pack the global gradient w_{r+1} and reward information into a new block, and then broadcast this new block. After receiving this new block, other miners will immediately stop the current hash calculation, and append the new block to their blockchain copies, once the validity of the new block is verified. Then, it will enter the next communication round. Again, please recall Assumption 2, with this setting, at the end of a communication round, the blockchain will only generate one block, and the blockchain copies of all miners will be the same, which means that we avoid the blockchain forking, thus there is no need to resolve ledger conflicts while reducing the risk of gradient abandonment

and consensus delay. According to Equation (4), the hash value will be calculated several times until *Target* is met, and the time of the hash calculation is related to the length of the string. Based on above discussion, the time complexity is $\mathcal{O}(n)$. We record the time cost here as \mathcal{T}_{bl} , which can be more significant compared with others.

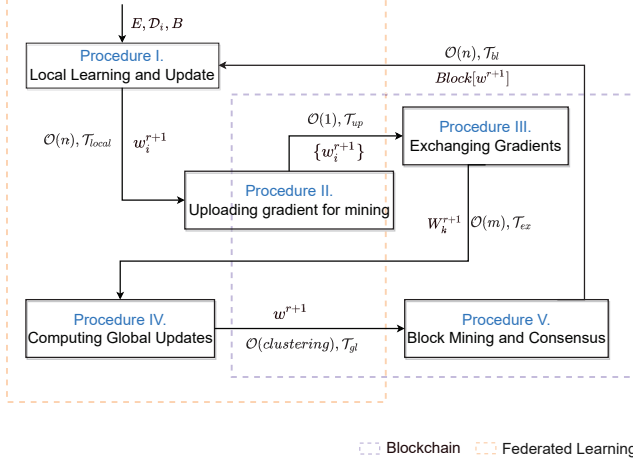


Figure 3: The Coupling structure and complexity of FAIR-BFL

4.6 Approximate Performance of FAIR-BFL

As shown Figure 3, the aforementioned five procedures are tightly coupled to form FAIR-BFL.

Flexibility Guarantee If we remove the Procedure-I and Procedure-IV, then FAIR-BFL boils down to a pure blockchain algorithm (see dashed purple rectangle, Figure 3). On the contrary, if we remove Procedure-III and Procedure-V, it will be equivalent to the pure FL algorithm (see dashed orange rectangle, Figure 3). This scale back functionality by design enables us to easily compare the performance and delay of those three approaches under the same setup using the same data set for their comparison. Moreover, we develop analytic model to quantify this flexibility and analyse the delay of the system Figure 3.

Approximate Performance Analysis The interactions in Figure 3 are explained as follows. Procedure-I receives the initial parameters and data set, executes in parallel on each client, and after a delay \mathcal{T}_{local} it eventually returns the local gradient w_{r+1}^i for a particular client. Procedure-II runs on each miner, receives w_{r+1}^i from the associated client, and spends \mathcal{T}_{up} time to return the gradient set $\{w_{r+1}^i\}$. After that, Procedure-III receives the gradient set $\{w_{r+1}^i\}$ of all miners and then waits for \mathcal{T}_{ex} time to get the complete local gradient set W_{r+1}^k . Procedure-IV uses W_{r+1}^k to calculate the global update w^{r+1} of this round, and the time \mathcal{T}_{gl} consumed depends on the clustering algorithm used. Procedure-V packs the global gradient w^{r+1} and generates $Block(Trans., w_{r+1})$,

where the above discussion has determined that the delay here is \mathcal{T}_{bl} . Therefore, the overall complexity of FAIR-BFL is close to $\mathcal{O}(n)$, while with n workers and m miners, the overall delay is $T_{(n,m)} = \mathcal{T}_{local} + \mathcal{T}_{up} + \mathcal{T}_{ex} + \mathcal{T}_{gl} + \mathcal{T}_{bl}$, which is compatible with vanilla BFL, so it can quickly learn from [21] to optimize the block arrival rate to obtain the best delay.

5 EVALUATION AND DISCUSSION

In this section, we conducted a series of experiments to comprehensively evaluate the performance of FAIR-BFL on real data set, Then we reported the changes in performance and delay under various conditions by adjusting parameters. At last, some novel insights such as the trade-off between performance and latency are presented.

5.1 Experimental setup

Our baseline methods for comparison include the Blockchain, FedAvg [15], and the state-of-the-art FL algorithm FedProx [9]. Then, we compare the performance of FAIR-BFL and baselines on the benchmark data set MNIST. The metrics for comparison are the average delay and the average performance. We calculate the average delay by $\sum_{i=1}^r d_i/r$, and the average accuracy by $\sum_{i=1}^n acc_i/n$, where d_i represents the delay of the communication round i , acc_i is the verification accuracy of client C_i in a communication round.

By default, we assign data to clients following the non-IID dynamics, and we set $n = 100$ and $m = 2$, $\eta = 0.01$, $E = 5$, and $B = 10$, respectively.

5.2 Performance Impact

For all experiments, We consider the model as converged when the accuracy in change is within 0.5% for 5 consecutive communication rounds, and perform 100 communication rounds by default.

5.2.1 General analysis of latency and performance. Figure 4 shows the simulation results of the general delay and performance. As shown in Figure 4a, the average delay of FAIR-BFL is between blockchain and FedAvg, rather than above the blockchain. This implies that Assumptions 1 and 2 can effectively reduce the BFL delay. In addition, from Figure 4b, FAIR-BFL has almost the same model performance as the FedAvg. FedProx has a lower accuracy than FAIR-BFL, and the accuracy still fluctuates after the model converges, which is because it uses the inexact solution to speed up the convergence.

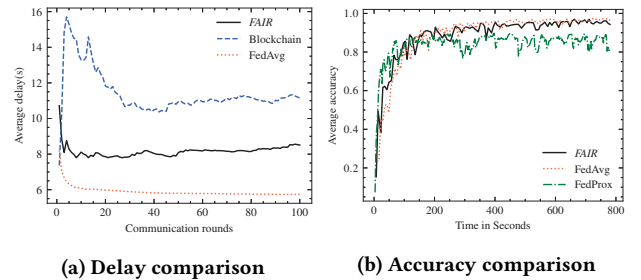


Figure 4: General comparison of FAIR-BFL and baselines

5.2.2 Impact of the Learning rate. We conducted multiple experiments, where $\eta \in [0.01, 0.05, 0.10, 0.15, 0.20]$. The result is shown in Figure 5. From Figure 5a, we can see that the effect of the learning rate on the average delay for *FAIR-BFL* and *FedAvg* is negligible, and we attribute it to the distributed (parallel) learning method. It is interesting to note that *FedProx* peaks at the beginning, which implies that it may need a larger η . Although there is no obvious impact on the delay, the accuracy is very different, as shown in Figure 5b. For *FAIR-BFL* and *FedAvg*, there is an optimal η such that the average accuracy is the highest. For *FedProx*, the learning rate does not significantly affect the average accuracy. To this end, we have the following insights.

Insight 1: Due to the benefits of distributed learning, we set the best learning rate in BFL to ensure the model performance. The delay overhead for this is acceptable.

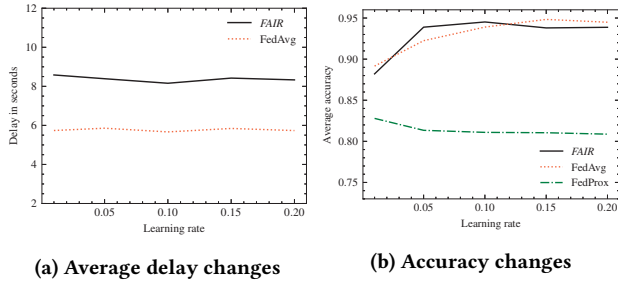


Figure 5: Performance and delay under various learning rates

5.2.3 Impact of the number of workers. The increase in the number of workers will lead to an increase in transactions, thus impacting the delay. Figure 6a shows the delay changes in this case. We can see that with the increase in the number of workers n , the delay of blockchain increases, and this is because the total number of new transactions is rising, while the block size is fixed. When a block cannot contain all transactions, transaction queuing will occur, which is regarded as a scalability issue [25] in blockchain. Please note that when the number of new transactions is much smaller than the block size, the delay caused by the increase of the clients will be minimal, such as the curve in interval $n \in [20, 100]$; when the total size of new transactions crosses the block size ($n \geq 100$), the delay caused by queuing will become more apparent, eventually making the delay of blockchain greater than the delay of *FAIR-BFL*, which is consistent with the result of Section 5.2.1. On the contrary, *FAIR-BFL* achieves a delay similar to *FedAvg*, It is almost unaffected by the number of clients. Thanks to Assumptions 1 and 2, no matter how many clients there are, there will be no queuing, because each block only contains the global gradient of the current round.

Insight 2: The block size will significantly affect the delay in large-scale scenarios. Assumptions 1 and 2 provide an effective way to solve this problem.

5.2.4 Impact of the number of miners. In contrast to Figure 6a, we set the number of clients to 100 and increase the number of miners to fully observe the impact of this change on delay in Figure 6b. It

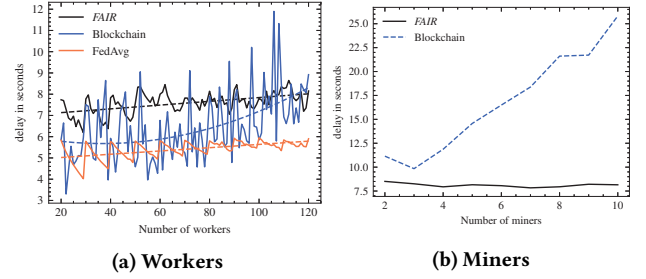


Figure 6: Average delay changes with the number of workers and miners

can be seen that in blockchain, the delay increases approximately exponentially as the number of miners increases. Because when more and more nodes participate in the mining competition, the probability of forking will significantly increase, which will take more time to merge conflicts. For *FAIR-BFL*, this issue is avoided due to Assumptions 1 and 2. Therefore, the increase in the number of miners does not significantly increase the delay.

Insight 3: Too many miners may cause delay, so the number of miners should be set appropriately. In BFL, we can alleviate this issue by Assumptions 1 and 2.

5.3 Cost-effectiveness

Here, we observe how Algorithm 2 with discarding strategy affects the delay, the accuracy and the convergence rate of *FAIR-BFL*. We use *DBSCAN* as the default clustering algorithm. Note that *FedProx* also drops clients to improve both the convergence rate and the model accuracy. However, *FedProx* avoids the global model skew by discarding stragglers, while we discard the low-contributing clients implied by the clustering algorithm. To demonstrate the effectiveness of our contribution-based incentive mechanism, we set the *drop_percent* of *FedProx* to 0.02 as a new baseline for comparison.

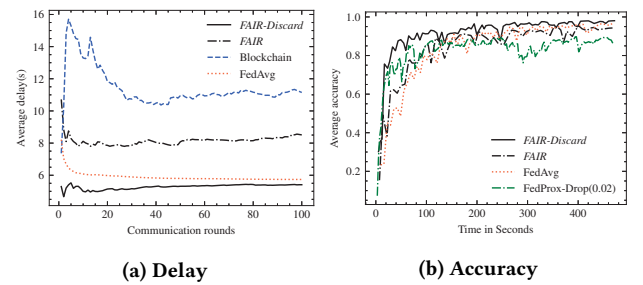


Figure 7: FAIR-BFL is faster without reducing accuracy

Then in Figure 7, we observe the difference in accuracy and delay with and without the discarding strategy, respectively. It can be seen from Figure 7a that the discarding strategy significantly reduces the average delay, even lower than that of *FedAvg*. The reason is that those workers with lower contributions no longer participate in the current communication round, which means fewer

workers and local gradients. On the one hand, fewer workers reduce the time cost for local updates and upload gradients and reduce the total number of communications, thus reducing costs. On the other hand, fewer local gradients accelerate the updates exchange and global aggregation, thus reducing the size of data packets in the network, to save the traffic and reduce the channel delays.

More importantly, the model converges better and faster so that the *FAIR-BFL* with discarding strategy in Figure 7b lies above the *FedAvg* and the original *FAIR* and reaches the convergence point between 250 and 300 seconds. Although *FedProx* also converges better initially, its accuracy stabilizes around 84%, which is lower than *FAIR-BFL*. The reason is that the low-contributing clients no longer participate in global aggregation, thus reducing the noise from low-quality data, effectively preventing the global model from falling into local optimal points, and improving the accuracy. As discussed above and shown in Figure 7a, the discarding strategy significantly reduces the average delay, and further reduces the time to reach the convergence. In conclusion, above results confirm that *FAIR-BFL* is more economic and faster.

Insight 4: Use the discarding strategy in large-scale scenarios to speed up model convergence and reduce the cost of communications and traffic.

Table 2: Detecting malicious attacks using our contribution-based incentive mechanism

Distribution	Round	Attacker Index	Drop Index	Detection Rate
Non-IID	1	[3, 7]	[2, 4, 5, 6]	0%
	2	[3, 6, 2]	[2, 6]	66.66%
	3	[6, 4, 7]	[4, 6]	66.66%
	4	[1, 6, 0]	[6]	33%
	5	[2, 8, 0]	[0, 8]	66.66%
	6	[7, 0]	[0, 7]	100%
	7	[0]	[0]	100%
	8	[3, 9]	[3]	50%
	9	[6, 0, 8]	[0, 8]	66.66%
	10	[6, 5]	[5, 6]	100%
Average Detection Rate				64.96%
IID	1	[0, 6, 1]	[0, 1]	66.66%
	2	[0, 3, 6]	[3, 6, 8]	66.66%
	3	[9]	[9]	100%
	4	[2]	[2]	100%
	5	[6, 3, 1]	[1, 3]	66.66%
	6	[5, 9]	[5]	50%
	7	[3]	[3]	100%
	8	[7, 0]	[7]	50%
	9	[1, 7, 2]	[1, 7]	66.66%
	10	[9]	[9]	100%
Average Detection Rate				75%

5.4 Security by design

In Section 5.3, we have shown that implementing Algorithm 2 with a discarding strategy for client selection is effective. Here, we will demonstrate its security. We set malicious nodes, which modify the actual local gradients to skew the global model. At the same time, *DBSCAN* is also adopted to find the difference in contribution. There are 10 indexed clients, and in each communication

round, randomly designate 1 to 3 clients as malicious nodes, and 10 rounds are executed in total, as shown in Table 2.

We can see that when there are few malicious nodes (1 malicious node in this experiment), the detection rate almost always reaches 100%, and *FAIR-BFL* identifies the forged gradients as with the low contributions, e.g., in the communication round 7. It means that with the vast majority of nodes remaining honest, the behavior of the malicious nodes is evident, because the modified local gradients are distant from the normal ones. As the number of malicious nodes increase, some forged gradients successfully cheat this mechanism, so the detection rate decreases, because anomalies that are obvious enough may mask those that are not obvious. Even so, the detection rate is maintained at an optimistic level, for example, in round 9. We also found that the average detection rate is higher in the case of IID, which is attributed to the fact that a good distribution of data makes the normal gradients more spatially concentrated and therefore easier to discover anomalies. Interestingly, in general, the detection rate increases as the model converges. The reason is that as the model converges, individual local gradients are getting similar. The results and the above discussion indicate that *FAIR-BFL* can resist malicious attacks to the greatest extent even in the case of non-IID.

Let's recall the major design aspects considered in *FAIR-BFL* to ensure security: i) we use the RSA algorithm to sign the local gradient to avoid modification during the upload process (see Figure 2). ii) the data recorded on the blockchain is immutable; iii) we use Algorithm 2 to reveal the contribution differences among nodes and discard low contributing local gradients (forged gradients) to resist malicious attacks; iv) we do not record any local gradients in the blockchain, so all nodes cannot observe and exploit this information (see Assumption 2). Thus, *FAIR-BFL* provides the privacy and security guarantee by design for the whole system dynamics.

6 CONCLUSION

We present a new research problem and develop valuable insights toward modelling blockchain-based federated learning. *FAIR-BFL* comes with a modular design that can dynamically scale functions according to the adopter's needs, thus providing unprecedented flexibility. Moreover, we probably alleviate the impending challenges of the vanilla BFL in terms of adjusting delay, performance, and aggregation by tight coupling blockchain and FL and fairness aggregation. This is one of the first attempts to redefine the block's data scope in BFL in order to prevent clients from observing others' gradients, thus enhancing privacy and security. More importantly, *FAIR-BFL* motivates all clients to contribute actively by identifying the client's contribution and issuing uneven rewards. Our experimental results show that *FAIR-BFL* can achieve desirable performance beyond the capacity of existing approaches. Furthermore, *FAIR-BFL* that employs the discarding strategy can naturally reap the benefits of privacy, malicious attack resistance, and client selection.

ACKNOWLEDGMENTS

This research is supported by the National Natural Science Fund of China (Project No. 71871090), and Hunan Provincial Science & Technology Innovation Leading Project (2020GK2005).

A PROOF OF THEOREM 3.1

As mentioned earlier, w_r^i is the local gradient of the client C_i at communication round r . For tracking the learning process at each local epoch, we use the notion of global epoch and $\mathcal{I}_E = \{nE \mid n = 1, 2, \dots, n\}$. For convenience, we denote by C_r is the most recent set of clients (with size K) selected in the communication round r . Note that C_r results from the random selection, and ergodicity comes from the stochastic gradients. So we slightly abuse the notation $\mathbb{E}_{C_r}(\cdot)$, taking the expectation means that we eliminate the former kind of randomness.

With \bar{w}_{r+1} denoting the global gradient at round $r+1$ and \bar{v}_{r+1} tracking the weighted average of all client-side gradients, we can see that \bar{w}_{r+1} is unbiased. In particular, $\bar{w}_{r+1} = \bar{v}_{r+1}$. Now, we formulate the following Lemma A.1 to bound the variance of \bar{w}_r .

LEMMA A.1. *For $r+1 \in \mathcal{I}_E$, if η_r is non-increasing and $\eta_r \leq 2\eta_{r+E}$ for all $r \geq 0$, then the expected difference between \bar{v}_{r+1} and \bar{w}_{r+1} is*

$$\mathbb{E}_{C_r} \|\bar{v}_{r+1} - \bar{w}_{r+1}\|^2 \leq \frac{4}{K} \eta_r^2 E^2 G^2$$

We first provide the proof of Lemma A.1 which builds the foundation for proving Theorem 3.1.

PROOF. Taking expectation over C_{r+1} , we have

$$\begin{aligned} \mathbb{E}_{C_r} \|\bar{w}_{r+1} - \bar{v}_{r+1}\|^2 &= \mathbb{E}_{C_r} \frac{1}{K^2} \sum_{l=1}^K \left\| v_{r+1}^l - \bar{v}_{r+1} \right\|^2 \\ &= \frac{1}{K} \sum_{k=1}^n p_i \left\| v_{r+1}^k - \bar{v}_{r+1} \right\|^2 \end{aligned}$$

where the first equality follows from v_{r+1}^i are independent and unbiased. Since $r+1 \in \mathcal{I}_E$, the time $r_0 = r - E + 1 \in \mathcal{I}_E$ is the underlying communication time, which implies $\{w_{r_0}^k\}_{k=1}^n$ are identical. Furthermore,

$$\begin{aligned} \sum_{i=1}^n p_i \|v_{r+1}^i - \bar{v}_{r+1}\|^2 &= \sum_{i=1}^n p_i \left\| (v_{r+1}^i - \bar{w}_{r_0}) - (\bar{v}_{r+1} - \bar{w}_{r_0}) \right\|^2 \\ &\leq \sum_{i=1}^n p_i \|v_{r+1}^i - \bar{w}_{r_0}\|^2 \end{aligned}$$

where the last inequality results from

$$\sum_{i=1}^n p_i (v_{r+1}^i - \bar{w}_{r_0}) = \bar{v}_{r+1} - \bar{w}_{r_0}$$

and

$$\mathbb{E} \|x - \mathbb{E}x\|^2 \leq \mathbb{E} \|x\|^2.$$

Therefore

$$\begin{aligned} \mathbb{E}_{C_r} \|\bar{w}_{r+1} - \bar{v}_{r+1}\|^2 &\leq \frac{1}{K} \sum_{i=1}^n p_i \mathbb{E} \|v_{r+1}^i - \bar{w}_{r_0}\|^2 \\ &\leq \frac{1}{K} \sum_{i=1}^n p_i \mathbb{E} \|v_{r+1}^i - w_{r_0}^i\|^2 \\ &\leq \frac{1}{K} \sum_{i=1}^n p_i E \sum_{t=r_0}^r \mathbb{E} \left\| \eta_t \nabla F_i(w_t^i, b) \right\|^2 \\ &\leq \frac{1}{K} E^2 \eta_{r_0}^2 G^2 \leq \frac{4}{K} \eta_r^2 E^2 G^2 \end{aligned}$$

□

As shown in Section 4.4 we adopt the partial aggregation and therefore the temporal evolution follow

$$\begin{aligned} v_{r+1}^i &= w_r^i - \eta_i \nabla F_i(w_r^i; b) \\ w_{r+1}^i &= \begin{cases} v_{r+1}^i & \text{if } r+1 \notin \mathcal{I}_E \\ \text{samples } C_r \text{ and average } \{v_{r+1}^i\} & \text{if } r+1 \in \mathcal{I}_E. \end{cases} \end{aligned}$$

Nex, we have

$$\begin{aligned} \|\bar{w}_{r+1} - w^*\|^2 &= \|\bar{w}_{r+1} - \bar{v}_{r+1} + \bar{v}_{r+1} - w^*\|^2 \\ &= \underbrace{\|\bar{w}_{r+1} - \bar{v}_{r+1}\|^2}_{A_1} + \underbrace{\|\bar{v}_{r+1} - w^*\|^2}_{A_2} \\ &\quad + 2 \underbrace{\langle \bar{w}_{r+1} - \bar{v}_{r+1}, \bar{v}_{r+1} - w^* \rangle}_{A_3} \end{aligned}$$

Considering unbiasedness of \bar{w}_{r+1} , A_3 will be vanished when we take expectation over C_{r+1} . If $r+1 \notin \mathcal{I}_E$, A_1 vanishes since $\bar{w}_{r+1} = \bar{v}_{r+1}$. Using Lemma A.1 to bound A_2 , we get

$$\mathbb{E} \|\bar{w}_{r+1} - w^*\|^2 \leq (1 - \eta_r \mu) \mathbb{E} \|\bar{w}_r - w^*\|^2 + \eta_r^2 B.$$

When $r+1 \in \mathcal{I}_E$, A_1 , we apply Lemma A.1 to bound A_1 and then

$$\begin{aligned} \mathbb{E} \|\bar{w}_{r+1} - w^*\|^2 &= \mathbb{E} \|\bar{w}_{r+1} - \bar{v}_{r+1}\|^2 + \mathbb{E} \|\bar{v}_{r+1} - w^*\|^2 \\ &\leq (1 - \eta_r \mu) \mathbb{E} \|\bar{w}_r - w^*\|^2 + \eta_r^2 (B + C) \end{aligned} \quad (5)$$

where

$$C \geq \frac{1}{\eta_r^2} \mathbb{E}_{C_r} \|\bar{v}_{r+1} - \bar{w}_{r+1}\|^2.$$

Equation (5) recursively portrays the distance between \bar{w}_{r+1} and w^* , and we will show how it is a decreasing function. Let $\Delta_r = \mathbb{E} \|\bar{w}_r - w^*\|^2$, Equation (5) can be simplified to

$$\Delta_{r+1} \leq (1 - \eta_r \mu) \Delta_r + \eta_r^2 (B + C) \quad (6)$$

For decreasing stepsize $\eta_r = \frac{\beta}{r+\gamma}$, we need $\beta > \frac{1}{\mu}$ and $\gamma > 0$. $\eta_1 \leq \min\{\frac{1}{\mu}, \frac{1}{4L}\} = \frac{1}{4L}$ and $\eta_r \leq 2\eta_{r+E}$ is an important condition for Equation (6). Therefore, we can see

$$\Delta_{r+1} \leq \frac{v}{\gamma + r} \quad (7)$$

when

$$v = \max \left\{ \frac{\beta^2 (B + C)}{\beta \mu - 1}, (\gamma + 1) \|w_1 - w^*\|^2 \right\}.$$

Now we use mathematical induction. When $r = 1$, Equation (7) holds from the definition of v . Assuming that the conclusion holds for some r , then at $r+1$,

$$\begin{aligned} \Delta_{r+1} &\leq (1 - \eta_r \mu) \Delta_r + \eta_r^2 B \\ &\leq \left(1 - \frac{\beta \mu}{r + \gamma}\right) \frac{v}{r + \gamma} + \frac{\beta^2 B}{(r + \gamma)^2} \\ &= \frac{r + \gamma - 1}{(r + \gamma)^2} v + \left[\frac{\beta^2 B}{(r + \gamma)^2} - \frac{\beta \mu - 1}{(r + \gamma)^2} v \right] \\ &\leq \frac{v}{r + \gamma + 1} \end{aligned}$$

Using strong convexity of $F(\cdot)$,

$$\mathbb{E}[F(\bar{\mathbf{w}}_r)] - F^* \leq \frac{L}{2} \Delta_r \leq \frac{L}{2} \frac{v}{\gamma + r}.$$

When $\beta = \frac{2}{\mu}$, $\gamma = \max\left\{8\frac{L}{\mu}, E\right\} - 1$ and with $\kappa = \frac{L}{\mu}$, we have $\eta_r = \frac{2}{\mu} \frac{1}{\gamma + r}$, which satisfies $\eta_r \leq 2\eta_{r+E}$. Therefore,

$$\mathbb{E}[F(\bar{\mathbf{w}}_r)] - F^* \leq \frac{\kappa}{\gamma + r} \left(\frac{2(B+C)}{\mu} + \frac{\mu(\gamma+1)}{2} \|\mathbf{w}_1 - \mathbf{w}^*\|^2 \right)$$

This proves Theorem 3.1.

REFERENCES

- [1] Sana Awan, Fengjun Li, Bo Luo, and Mei Liu. 2019. Poster: A Reliable and Accountable Privacy-Preserving Federated Learning Framework using the Blockchain. In *Proceedings of the 2019 ACM SIGSAC Conference on Computer and Communications Security (CCS '19)*. Association for Computing Machinery, New York, NY, USA, 2561–2563. <https://doi.org/10.1145/3319535.3363256>
- [2] Xianglin Bao, Cheng Su, Yan Xiong, Wenchao Huang, and Yifei Hu. 2019. FLChain: A Blockchain for Auditable Federated Learning with Trust and Incentive. In *2019 5th International Conference on Big Data Computing and Communications (BIGCOM)*. 151–159. <https://doi.org/10.1109/BIGCOM.2019.00030>
- [3] Bin Cao, Yixin Li, Lei Zhang, Long Zhang, Shahid Mumtaz, Zhenyu Zhou, and Mugen Peng. 2019. When Internet of Things Meets Blockchain: Challenges in Distributed Consensus. *IEEE Network* 33, 6 (Nov. 2019), 133–139. <https://doi.org/10.1109/MNET.2019.1900002>
- [4] Jianmin Chen, Xinghao Pan, Rajat Monga, Samy Bengio, and Rafal Jozefowicz. 2017. Revisiting Distributed Synchronous SGD. *arXiv:1604.00981 [cs]* (March 2017). <http://arxiv.org/abs/1604.00981>
- [5] Yae Jee Cho, Jianyu Wang, and Gauri Joshi. 2022. Towards Understanding Biased Client Selection in Federated Learning. In *Proceedings of The 25th International Conference on Artificial Intelligence and Statistics*. PMLR, 10351–10375. <https://proceedings.mlr.press/v151/jee-cho22a.html> ISSN: 2640-3498.
- [6] Matt Fredrikson, Somesh Jha, and Thomas Ristenpart. 2015. Model Inversion Attacks that Exploit Confidence Information and Basic Countermeasures. In *Proceedings of the 22nd ACM SIGSAC Conference on Computer and Communications Security (CCS '15)*. Association for Computing Machinery, New York, NY, USA, 1322–1333. <https://doi.org/10.1145/2810103.2813677>
- [7] Hyesung Kim, Jihong Park, Mehdi Bennis, and Seong-Lyun Kim. 2020. Blockchain On-Device Federated Learning. *IEEE Communications Letters* 24, 6 (June 2020), 1279–1283. <https://doi.org/10.1109/LCOMM.2019.2921755>
- [8] Jakub Konečný, H. Brendan McMahan, Daniel Ramage, and Peter Richtárik. 2016. Federated Optimization: Distributed Machine Learning for On-Device Intelligence. *arXiv:1610.02527 [cs]* (Oct. 2016). <http://arxiv.org/abs/1610.02527>
- [9] Tian Li, Anit Kumar Sahu, Manzil Zaheer, Maziar Sanjabi, Ameet Talwalkar, and Virginia Smith. 2020. Federated optimization in heterogeneous networks. In *Proceedings of machine learning and systems*, I. Dhillon, D. Papailiopoulos, and V. Sze (Eds.), Vol. 2. 429–450.
- [10] Xiang Li, Kaixuan Huang, Wenhao Yang, Shusen Wang, and Zhihua Zhang. 2020. On the convergence of FedAvg on non-iid data. In *8th international conference on learning representations, ICLR 2020, addis ababa, ethiopia, april 26-30, 2020*. OpenReview.net. <https://openreview.net/forum?id=HJxNAnVtDS>
- [11] Yuzheng Li, Chuan Chen, Nan Liu, Huawei Huang, Zibin Zheng, and Qiang Yan. 2021. A Blockchain-Based Decentralized Federated Learning Framework with Committee Consensus. *IEEE Network* 35, 1 (Jan. 2021), 234–241. <https://doi.org/10.1109/MNET.011.2000263>
- [12] Yunlong Lu, Xiaohong Huang, Yueyue Dai, Sabita Maharjan, and Yan Zhang. 2020. Blockchain and Federated Learning for Privacy-Preserved Data Sharing in Industrial IoT. *IEEE Transactions on Industrial Informatics* 16, 6 (June 2020), 4177–4186. <https://doi.org/10.1109/TII.2019.2942190>
- [13] Chuan Ma, Jun Li, Ming Ding, Long Shi, Taotao Wang, Zhu Han, and H. Vincent Poor. 2021. When Federated Learning Meets Blockchain: A New Distributed Learning Paradigm. *arXiv:2009.09338 [cs]* (June 2021). <http://arxiv.org/abs/2009.09338>
- [14] Umer Majeed and Choong Seon Hong. 2019. FLchain: Federated Learning via MEC-enabled Blockchain Network. In *2019 20th Asia-Pacific Network Operations and Management Symposium (APNOMS)*. 1–4. <https://doi.org/10.23919/APNOMS.2019.8892848>
- [15] Brendan McMahan, Eider Moore, Daniel Ramage, Seth Hampson, and Blaise Agüera y Arcas. 2017. Communication-Efficient Learning of Deep Networks from Decentralized Data. In *Proceedings of the 20th International Conference on Artificial Intelligence and Statistics*. PMLR, 1273–1282. <https://proceedings.mlr.press/v54/mcmahan17a.html>
- [16] Milad Nasr, Reza Shokri, and Amir Houmansadr. 2019. Comprehensive Privacy Analysis of Deep Learning: Passive and Active White-box Inference Attacks against Centralized and Federated Learning. In *2019 IEEE Symposium on Security and Privacy (SP)*. 739–753. <https://doi.org/10.1109/SP.2019.00065>
- [17] Dinh C. Nguyen, Ming Ding, Quoc-Viet Pham, Pubudu N. Pathirana, Long Bao Le, Aruna Seneviratne, Jun Li, Dusit Niyato, and H. Vincent Poor. 2021. Federated Learning Meets Blockchain in Edge Computing: Opportunities and Challenges. *IEEE Internet of Things Journal* 8, 16 (Aug. 2021), 12806–12825. <https://doi.org/10.1109/JIOT.2021.3072611>
- [18] Shiva Raj Pokhrel. 2020. Federated learning meets blockchain at 6G edge: a drone-assisted networking for disaster response. In *Proceedings of the 2nd ACM MobiCom Workshop on Drone Assisted Wireless Communications for 5G and Beyond (DroneCom '20)*. Association for Computing Machinery, New York, NY, USA, 49–54. <https://doi.org/10.1145/3414045.3415949>
- [19] Shiva Raj Pokhrel. 2021. Blockchain Brings Trust to Collaborative Drones and LEO Satellites: An Intelligent Decentralized Learning in the Space. *IEEE Sensors Journal* 21, 22 (Nov. 2021), 25331–25339. <https://doi.org/10.1109/JSEN.2021.3060185> Conference Name: IEEE Sensors Journal.
- [20] Shiva Raj Pokhrel and Jinho Choi. 2020. A Decentralized Federated Learning Approach for Connected Autonomous Vehicles. In *2020 IEEE Wireless Communications and Networking Conference Workshops (WCNCW)*. 1–6. <https://doi.org/10.1109/WCNCW48565.2020.9124733>
- [21] Shiva Raj Pokhrel and Jinho Choi. 2020. Federated Learning With Blockchain for Autonomous Vehicles: Analysis and Design Challenges. *IEEE Transactions on Communications* 68, 8 (Aug. 2020), 4734–4746. <https://doi.org/10.1109/TCOMM.2020.2990686>
- [22] Rodrigo Roman, Jianying Zhou, and Javier Lopez. 2013. On the features and challenges of security and privacy in distributed internet of things. *Computer Networks* 57, 10 (July 2013), 2266–2279. <https://doi.org/10.1016/j.comnet.2012.12.018>
- [23] Sebastian U. Stich. 2019. Local SGD converges fast and communicates little. In *7th international conference on learning representations, ICLR 2019, new orleans, LA, USA, may 6-9, 2019*. OpenReview.net. <https://arxiv.org/abs/1805.09767>
- [24] Jianyu Wang, Qinghua Liu, Hao Liang, Gauri Joshi, and H. Vincent Poor. 2020. Tackling the Objective Inconsistency Problem in Heterogeneous Federated Optimization. In *Advances in Neural Information Processing Systems*, Vol. 33. Curran Associates, Inc., 7611–7623.
- [25] Kaiwen Zhang and Hans-Arno Jacobsen. 2018. Towards Dependable, Scalable, and Pervasive Distributed Ledgers with Blockchains. In *ICDCS*. 1337–1346.
- [26] Yuchen Zhang, Martin J Wainwright, and John C Duchi. 2012. Communication-efficient algorithms for statistical optimization. In *Advances in neural information processing systems*, F. Pereira, C. J. C. Burges, L. Bottou, and K. Q. Weinberger (Eds.), Vol. 25. Curran Associates, Inc. <https://doi.org/10.1109/cdc.2012.6426691>